Supplementary Information

Photo-induced removal of uranium under air without external photocatalysts

Zhe Wang[a], Bin Li[a], Hailin Shang[a], Xue Dong[b], Liqin Huang[b], Qi Qing[b], Chao Xu[b], Jing Chen[b], Hongtao Liu[d], Xiangke Wang[a], Xiao-Gen Xiong[c]*, Yuexiang Lu[b]**

[a]The MOE Key Laboratory of Resources and Environmental System Optimization, College of Environmental Science and Engineering, North China Electric Power University, Beijing 102206, P.R. China.

[b]Institute of Nuclear and New Energy Technology, Tsinghua University, Beijing 100084, P. R. China.

[c]Sino-French Institute of Nuclear Engineering and Technology, Sun Yat-sen University, Zhuhai, 519082, P. R. China

[d]Key Laboratory of Interfacial Physics and Technology, Shanghai Institute of Applied Physics, Chinese Academy of Sciences, University of Chinese Academy of Sciences, Shanghai, 201800, P. R. China.

Corresponding authors

*Email: xkwang@ncepu.edu.cn (X. Wang); xiongxg@mail.sysu.edu.cn (X.-G. Xiong); luyuexiang@mail.tsinghua.edu.cn (Y. Lu)

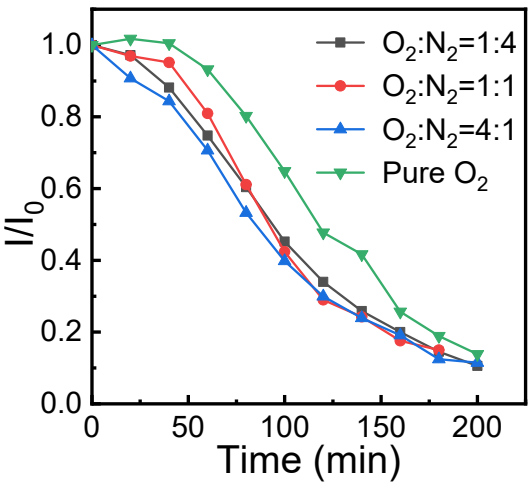

Fig. S1 The variation of uranium concentration along with the irradiation time under bubbling gas with different O_2/N_2 ratio.

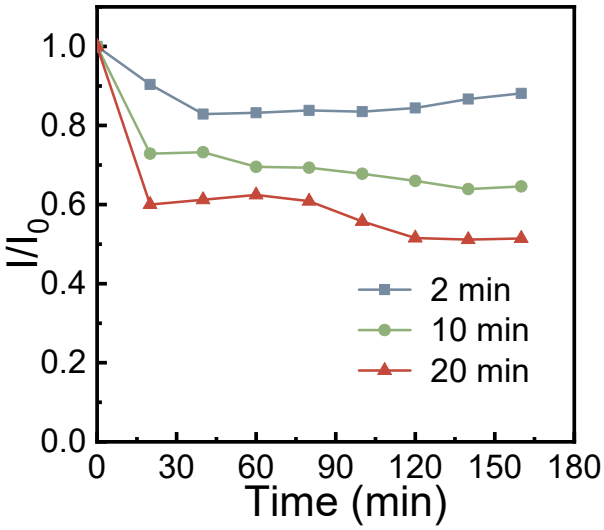

Fig. S2 The variation of uranium concentration after irradiated for 2 min, 10 min and 20 min under air atmosphere.

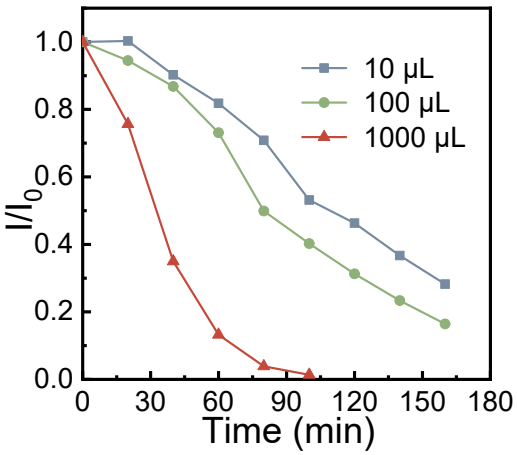

Fig. S3 The elimination of uranium by adding various amount of H_2O_2 solution directly to the solution.

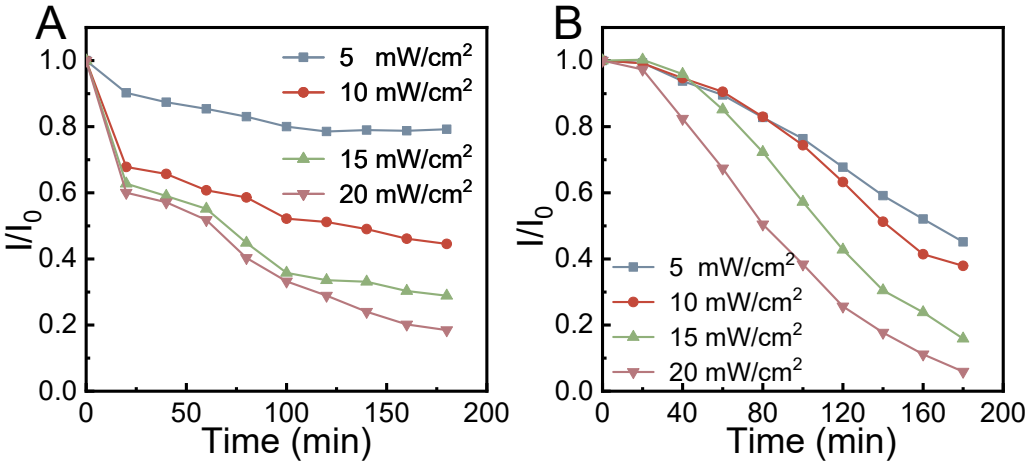

Fig. S4 The influence of light intensity on the elimination of uranium in (A) air and (B) N_2 atmosphere. [U]=0.4 mM，pH=5.

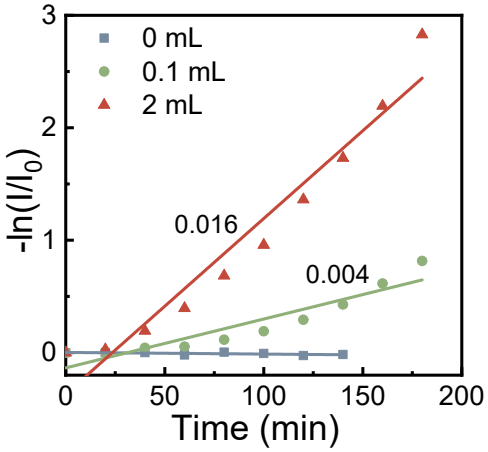

Fig. S5 The fitting reaction rate of uranium elimination with different amount of CH_3OH.

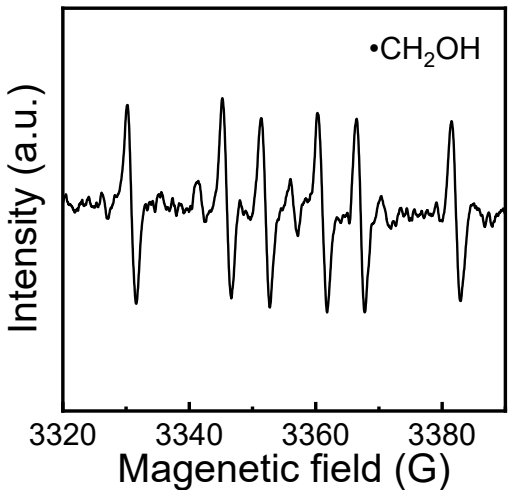

Fig. S6 The EPR spectra of uranium and methanol under simulated sunlight.

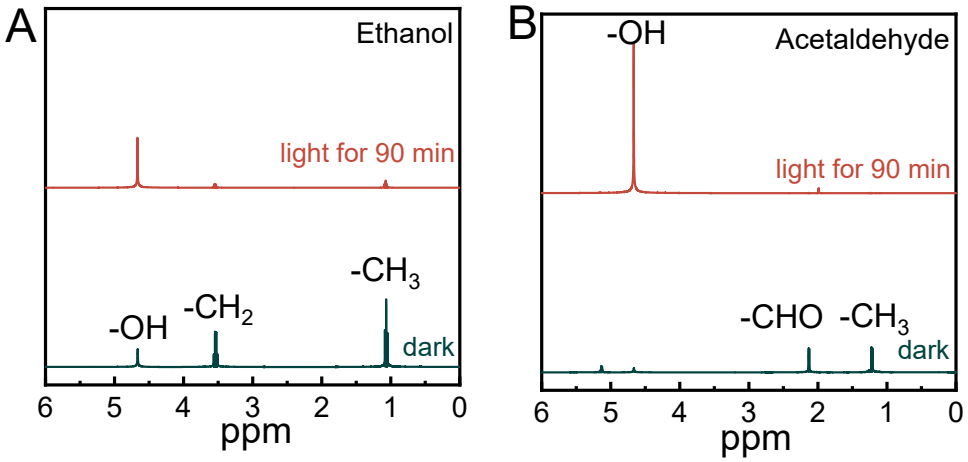

Fig. S7 The NMR spectra of (A) ethanol (B) acetaldehyde in uranium solution before and after irradiation.

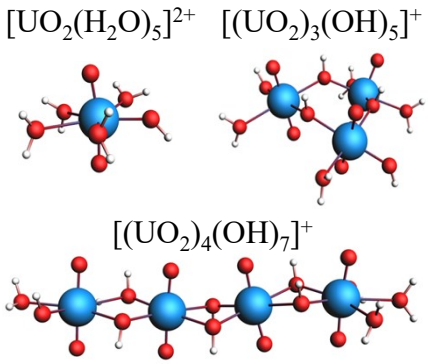

Fig. S8 The possible structures of the dominant uranium species at different pH.

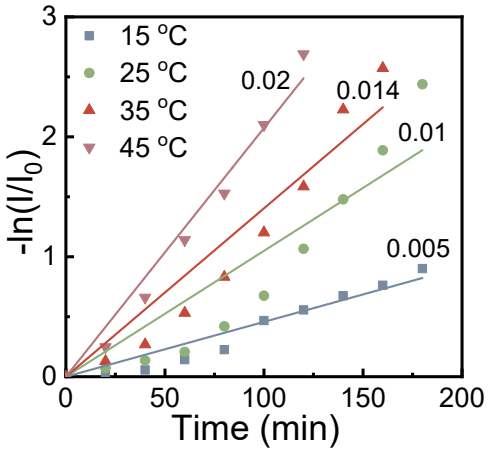

Fig. S9 The fitting reaction rate under different temperature. [U]=0.4 mM, pH=5.

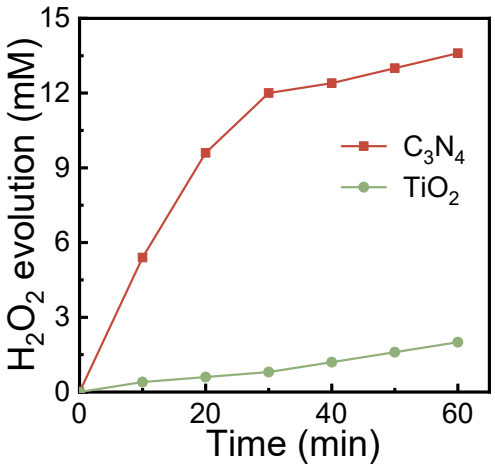

Fig. S10 The H_2O_2 evolution of C_3N_4 and TiO_2 with methanol under the irradiation of simulated sunlight.

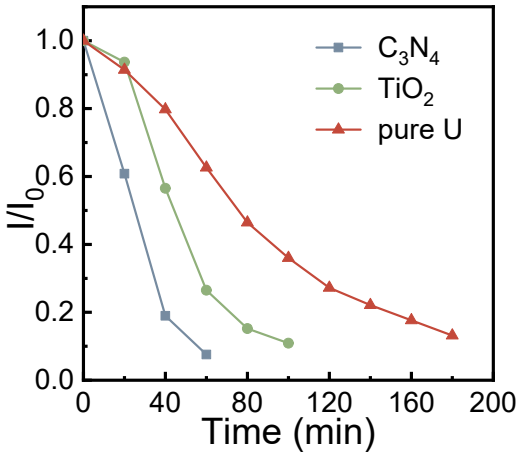

Fig. S11 The elimination of uranium with different catalysts under simulated sunlight.

Computational methods

We used both the relativistic density functional theory (DFT) and high-level wave function theory (WFT) to study the molecules investigated in this article. We carried out the DFT calculations with PBE exchange-correlation functional implemented in Amsterdam Density Functional (ADF 2016.01) to optimize the geometries and confirm the minimum through vibrational frequency calculations. In ADF calculations, the scalar-relativistic (SR) effects were handled through zero-order-regular approximation (ZORA), and the Slater basis sets with the quality of triple-ζ plus two polarization functions (TZ2P) were employed. In order to reduce the computational costs, the frozen core approximation was applied to the [$1s^2$-$5d^{10}$] for U, [$1s^2$] for O and [$1s^2$-$2p^6$] for Cl. The corrections of Grimme's D3BJ dispersion were also included to account for the dispersion-type interactions between the soft ligands. The solvation effects have been treated using the conductor-like screening model (COSMO), in which the Delly type of cavity implemented in ADF was used. We optimized all the ligands concerned in this article (H_2O, OH^-, OOH^-, NO_3^- and HCO_3^-) at the PBE-D3 level including the COSMO treatment to account for the solvation effects. The subsequent vibrational calculations were carried out to confirm the minimum of the optimized structures and calculate the Gibbs free energy. For large molecules with more than two uranyl units, we firstly optimized the geometry at the PBE-D3 level, then we performed the single-point calculation incorporating the COSMO treatment to account for the solvation effects. The solvation-effects corrected energies were further used for calculating the reaction heat.

For considering the stability of the ·(H-UO2+ 2), the sophisticated electron correlation calculations were also done to generate the accurate thermodynamic data. We optimized the geometries of the certain molecules at the CCSD(T) (coupled-cluster singles-and-doubles plus perturbative triples) level using Molpro 2020.2. In the Molpro calculations, the scalar-relativistic effects of uranium were considered through the pseudopotential approach, where the energy-consistent pseudopotential ECP60MDF

(U) of Stuttgart/Cologne group and the corresponding valence triple-ζ basis sets were used. The all-electron augmented triple-ζ basis sets aug-cc-pVTZ were used for light elements H an O.

T1. The decomposition reaction of ·(H-UO2+ 2)

As shown in **Fig. 3** of the article, one of new factors in our proposed reaction mechanism is that ·(H-UO2+ 2) generated in the photochemical reaction will split into H^+ and UO_2^+ rather than react with O_2 due to its inherent instability. In order to rationalize our proposed mechanism, we did the high-level theoretical calculations to predict the heat of the decomposition reaction of ·(H-UO2+ 2). The formation of O-H bond will apparently affect the interaction between uranium and two oxygen atoms. We optimized the geometries of both UO2+ 2 and ·(H-UO2+ 2) at the level of CCSD(T) (coupled-cluster singles-and-doubles plus perturbative triples) with triple-ζ basis sets. Our gas phase calculations show that UO2+ 2 has $D_{\infty h}$ symmetry with $^1\Sigma^+_g$ ground state, and the bond length of U≡O is 169.8 nm. ·(H-UO2+ 2)has $C_{\infty v}$ symmetry with $^2\Sigma^+$ ground state, while the two U-O bonds in ·(H-UO2+ 2) are 172.7 nm and 190.5 nm, respectively. This elongation of R(U-O) indicates the addition of H will significantly weaken the bonding between uranium and oxygen atoms. Due to the special affinity between uranium and oxygen, we consider the reformation of strong U≡O bond through the dehydrogenation reaction of ·(H-UO2+ 2) under aqueous solution. The split reaction is:

$$\cdot(\text{H-UO2+ 2}) + H_2O \rightarrow UO_2^+ + H_3O^+$$

Our CCSD(T) calculations suggest that ·(H-UO2+ 2) would split into UO2+ 2 and H^+ with the reaction energy of -3.98 kcal/mol, in which the solvation energies were considered with the calculated corrections from the incorporation of COSMO model within the scheme of density functional theory (DFT) using PBE exchange-correlation functional.

T2. Schematic of the energy profile of $[UO_2]^{2+}$ reacted with CH_3OH

In this work, we proposed that in a series of organic reactants, the H-atom binding to carbon rather than oxygen can be easily abstracted by the uranyl, and this assumption has been verified by the NMR experiments. Here we also used both the DFT and CCSD(T) calculations to theoretically predict the thermal effects of the proposed reactions. In order to reduce the computational costs, we only implicitly considered the solvation effects through the COSMO model as explained in the computational methods sections, and the energy profile presented in this section were based on the energies generated at the CCSD(T) level corrected by the solvation effects through COSMO calculations at the PBE-D3 level.

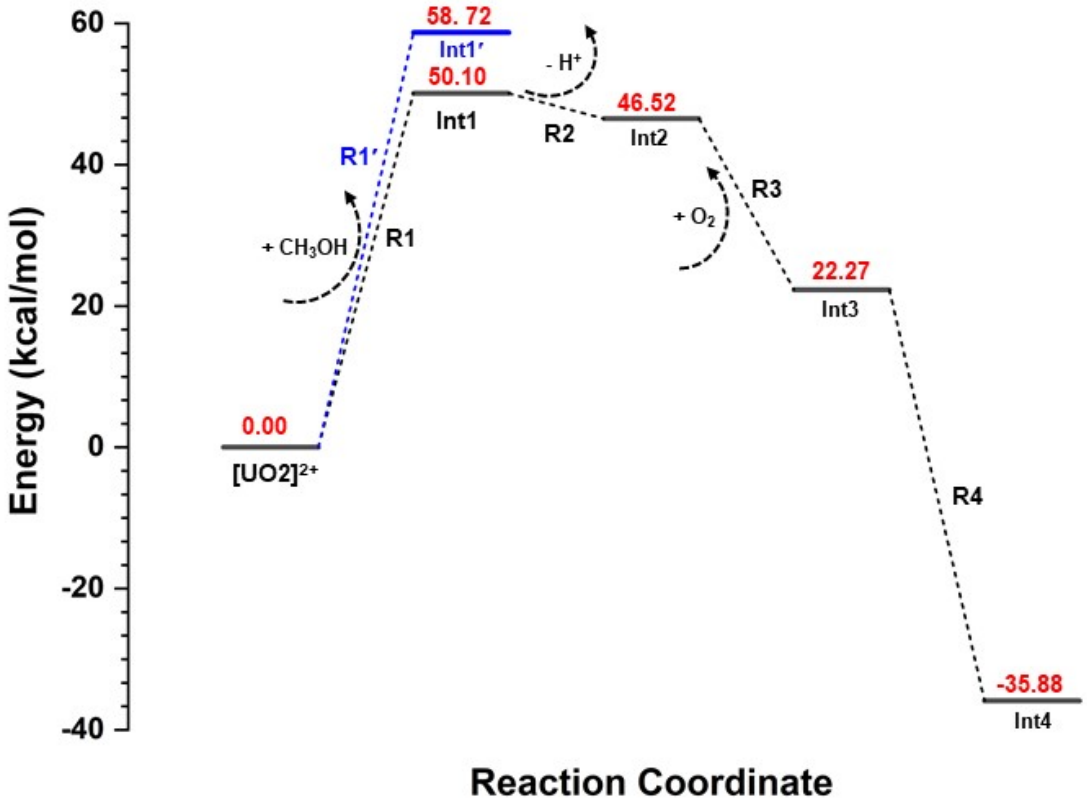

The reactions in the above graph including:

R1: $[UO_2]^{2+} + CH_3OH \rightarrow \cdot[OUOH]^{2+} + \cdot CH_2OH$, ΔE = 50.10 kcal/mol

R1′: $[UO_2]^{2+} + CH_3OH \rightarrow \cdot[OUOH]^{2+} + CH_3O\cdot$, ΔE = 58.72 kcal/mol

R2: $\cdot[OUOH]^{2+} + H_2O \rightarrow [UO_2]^{+} + H_3O^{+}$, ΔE = –3.58 kcal/mol

R3: $\cdot CH_2OH + O_2 \rightarrow CH_2O + \cdot OOH$, ΔE = –24.25 kcal/mol

R4: $\cdot CH_2OH + \cdot OOH \rightarrow CH_2O + H_2O_2$, ΔE = –58.15 kcal/mol

(Note: In this schematic energy profile, we neglected the oxidative conversion of $[UO_2]^+$ to $[UO_2]^{2+}$, and the photoexcitation of $[UO_2]^{2+}$ was also not included in the above graph.)

T3. Estimation of the binding strength between uranyl and ligands concerned in this article

In the aqueous condition, uranyl ion is stabilized through the coordination with the ligands in the solution, and the difference of the binding strength between the metal ion and ligands has significant effects over the reaction pathway. In our study, we mainly concern the following ligands: H_2O, OH^-, OOH^- and NO_3^-. Due to the very complicate surroundings of uranyl in the solution, it is very difficult to examine all possible existence of the cation in the solution. Therefore, the rudimentary strategy used in our investigation is that we consider the following formation reactions and calculate the change in Gibbs free energies at room temperature (T = 298.15 K):

$[UO_2]^{2+} + 5H_2O = [UO_2(H_2O)_5]^{2+}$ $\Delta G^0 = -25.57$ kcal/mol

$[UO_2]^{2+} + 3NO_3^- = [UO_2(NO_3)_3]^-$ $\Delta G^0 = -74.71$ kcal/mol

$[UO_2]^{2+} + 3OH^- = [UO_2(OH)_3]^-$ $\Delta G^0 = -144.38$ kcal/mol

$[UO_2]^{2+} + 3OOH^- = [UO_2(OOH)_3]^-$ $\Delta G^0 = -141.87$ kcal/mol

From the above theoretical results, we have a roughly estimation the studied ligands in this article bond to the cation in the order: $OH^- \sim OOH^- > \sim NO_3^- > H_2O$.

The optimized geometries of the studied uranium complexes are:

$[UO_2(H_2O)_5]^{2+}$ $[UO_2(OH)_3]^-$ $[UO_2(NO_3)_3]^-$ $[UO_2(OOH)_3]^-$

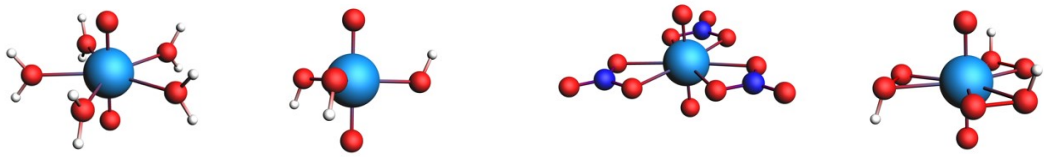

T4. The geometries and stability of polymeric uranyl complexes in aqueous solution

As indicated in the **Fig. 4c** of the article, at our experimental pH conditions, the main species of uranyl in the aqueous solution are $[UO_2(OH)_3]^-$, $[(UO_2)_3(OH)_5]^+$ and

$[(UO_2)_4(OH)_7]^+$. We optimize the possible dimeric, trimeric and tetrameric complexes in aqueous solution. The maximum coordination amount of uranyl on the equatorial plane is five, and due to the strong binding interaction between uranyl and OH^-, the anion can act as bridge when two uranyl connected. For dimeric uranyl complexes, we have following structures:

$[(UO_2)_2(H_2O)_8(OH)]^{3+}$ $[(UO_2)_2(H_2O)_6(OH)_2]^{2+}$

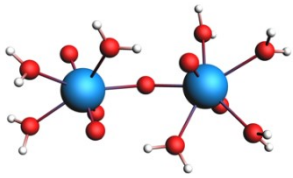
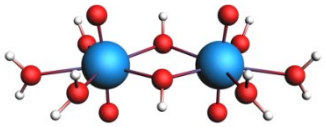

We also calculate the change of heat for the following reaction:

$$[(UO_2)_2(H_2O)_8(OH)]^{3+} + OH^- = [(UO_2)_2(H_2O)_6(OH)_2]^{2+} + 2H_2O$$

$$\Delta E = -44.64 \text{ kcal/mol}$$

For trimeric complexes, we calculated the following complexes:

$[(UO_2)_3(H_2O)_4(OH)_5]^+$		
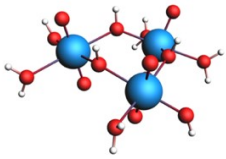		
$[(UO_2)_3(H_2O)_5(OH)_5]^+$		
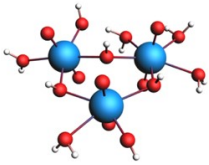	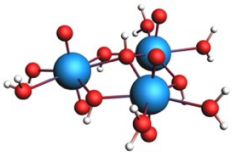	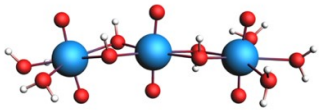
0.00 kcal/mol	3.53 kcal/mol	4.95 kcal/mol
$[(UO_2)_3(H_2O)_6(OH)_5]^+$		
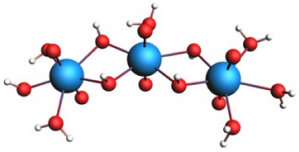	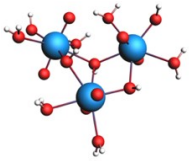	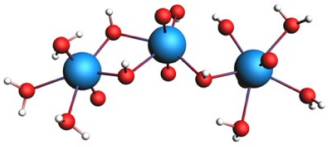
0.00 kcal/mol	0.58 kcal/mol	6.94 kcal/mol
$[(UO_2)_3(H_2O)_7(OH)_6]^+$		
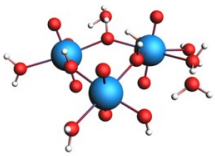		

And for tetrameric complexes:

$[(UO_2)_4(H_2O)_5(OH)_7]^+$	
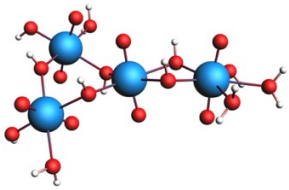	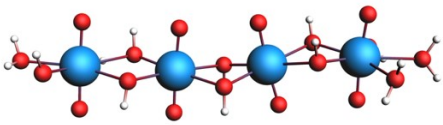
0.00 kcal/mol	0.21 kcal/mol
$[(UO_2)_4(H_2O)_6(OH)_7]^+$	
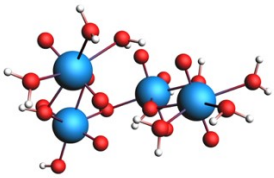	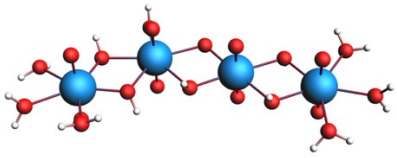
0.00 kcal/mol	6.91 kcal/mol
$[(UO_2)_4(H_2O)_7(OH)_7]^+$	
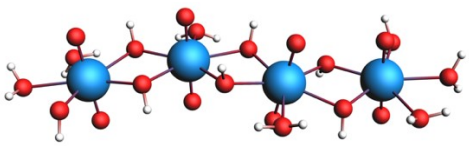	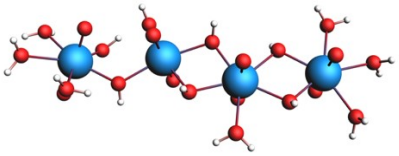
0.00 kcal/mol	4.40 kcal/mol
$[(UO_2)_4(H_2O)_8(OH)_7]^+$	
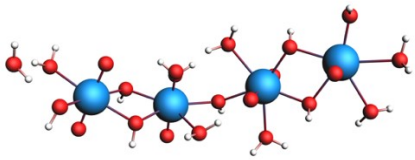	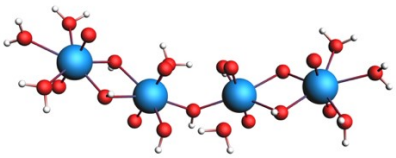
0.00 kcal/mol	8.25 kcal/mol

The theoretical calculations show that trimeric complexes prefer “cyclic” structures, while tetrameric complexes prefer “linear” structure.